The time reversed elastic nonlinearity diagnostic applied to evaluation of diffusion bonds

T. J. Ulrich,[1,a] Alexander M. Sutin,[2] Thomas Claytor,[3] Pallas Papin,[4] Pierre-Yves Le Bas,[1] and James A. TenCate[1]

[1]*EES-11, Los Alamos National Laboratory, Los Alamos, New Mexico 87545, USA*
[2]*Stevens Institute of Technology, Hoboken, New Jersey 07030, USA*
[3]*AET-6, Los Alamos National Laboratory, Los Alamos, New Mexico 87545, USA*
[4]*MST-6, Los Alamos National Laboratory, Los Alamos, New Mexico 87545, USA*

With the recent application of time reversed acoustics and nonlinear elasticity to imaging mechanical damage, the development of time reversal based nondestructive evaluation techniques has begun. Here, diffusion bonded metal disks containing intentionally disbonded regions are analyzed using the time reversed elastic nonlinearity diagnostic. The nonlinear results are compared with linear ultrasonic imaging (C scan). Scanning electron microscopy is shown to illustrate the differences between the features seen by the linear and nonlinear methods. © *2008 American Institute of Physics*. [DOI: 10.1063/1.2998408]

Time reversal (TR) techniques for wave propagation provide a means to focus energy at a defined time and space or at an unknown location[1,2] (i.e., source or scatterer not known *a priori*) without the need to calculate time delays, as is necessary for phased arrays. This is possible even when the TR mirror (TRM) has only a single element,[3,4] providing a sufficient amount of scattering takes places, and is consequently used in the back propagation. Combining this technique with the damage detection capabilities of nonlinear elasticity measurements,[5,6] methods for imaging mechanical damage in solids have been developed.[7–9]

Here we present a method to utilize a reverberant cavity and impulse responses to perform TR experiments in thin ($h \approx 5$ mm, $d \approx 5$ cm) diffusion bonded disks, in order to generate localized large amplitude signals for the purpose of probing for a nonlinear elastic response. To enhance our ability to detect the nonlinear response, we employ a technique used in landmine detection[10] and medical imaging,[11] which we refer to as phase inversion. The resulting nonlinear image is compared with that from a linear ultrasonic method (i.e., C scan) and destructive testing is performed to investigate the differences in the linear and nonlinear images.

To excite a localized region with as large an amplitude as possible, we have chosen to use a reverberant cavity. Attaching a reverberant cavity to our sample allows us to bond as many transducers as desired to the cavity, thus increasing our TR focal amplitudes by a factor of N ($N \equiv$ number of transducers). As the contact between the sample and transducers is defined by the contact area with the reverberant cavity (~ 4 cm^2), numerous transducers may be added to the reverberator without impinging upon the sample itself. The multiple scattering that occurs in the reverberator (a multi-faceted Al block) also adds to the effective aperture of the TRM, providing a strong focus at the point of detection on the sample of interest. With the source transducers fixed to the reverberator, and reverberator to the sample, the sample can then be scanned with a scanning laser vibrometer using

reciprocal TR (Ref. 2) to focus elastic energy at the laser vibrometer detection position.

To accomplish the task of using TR and phase inversion together experimentally, we have chosen to use an impulse response and phase inversion procedure inspired by a method used by Sutin *et al.*[10] for landmine detection. In this procedure the impulse response of the system (over a limited bandwidth) from each of the N transducers to the inspection point (i.e., laser vibrometer location) is acquired from the correlation of the response to a "chirp" source signal with the source function itself. These source impulse response functions are time reversed and broadcast in such a manner as to construct two TR focused signals, one from the impulse response and the other from the phase inverted impulse response. These two focused signals are contained consecutively in the measured signal $F(t)$. To spatially interrogate the sample, a collection of $F_j(t)$ are measured at j locations defined by the laser vibrometer detection points (e.g., M_x and M_y in Table I). Figure 1 displays the focused signals and the residual after the summation at two detection points [linear (a) and (c) and nonlinear (b) and (d)].

The above procedure provides us with a set of data (i.e., F_j) to be analyzed for the nonlinear response present in each signal, from which an image of the sample is created. In this procedure there are required parameters (such as the duration of the focused signals T and the frequency range of the chirp) that need to be defined to perform the tests. Presented here are the results from one set of parameters, given in Table I, though the possibilities for the variation in these parameters are endless and can be altered as best suit the experiment.

TABLE I. Experimental parameters.

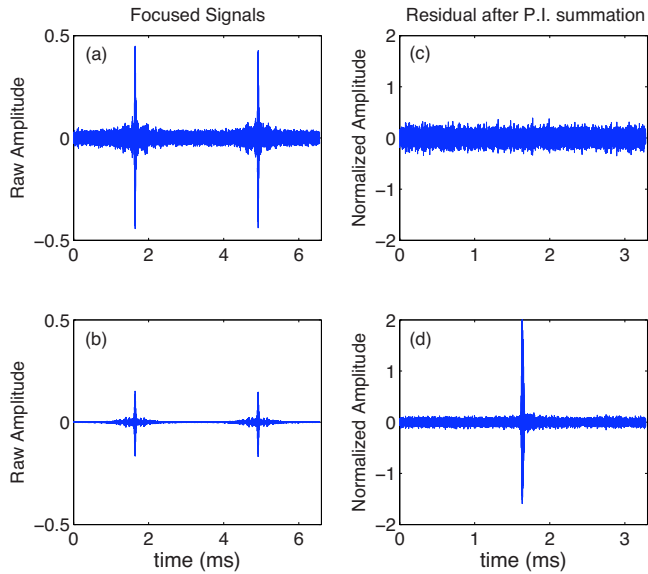| Parameter	Value
Chirp frequency band	150–250 kHz
T (duration of each F_j)	3.2768 ms
N (number of transducers)	8
$M_x \times M_y = M$	$51 \times 51 = 2601$
Δx and Δy (step size)	1 mm

[a]Electronic mail: tju@lanl.gov.

FIG. 1. (Color online) Comparison of signals with and without nonlinear content: (a) two consecutive TR focused signals (the second phase inverted with respect to the first) at a "linear" location, (b) two TR focused signals (the second phase inverted) at a "nonlinear" location, (c) summation of the two focused signals shown in (a), and (d) summation of the two focused signals shown in (b). Note the residual focus seen in (d), i.e., the nonlinear components. The residual signals (c) and (d) are normalized by the square of the focused signals in (a) and (b), respectively, as is necessary for proper analysis.

The frequency band chosen here was to maximize the efficiency of the available transducers and probe the material to a depth such that the bonded region of interest ($\sim$2.5 mm below the surface) is excited by the TR signal focused on the surface. All other parameters were chosen for convenience.

As stated above, each of the measured focused signals F_j contains two focused signals, that from the original impulse responses and the focus of the inverted impulse responses. The analysis required to produce an image from the set of focused signals F_j requires first that the two focused signals contained in F_j be separated, i.e.,

$$F_j^I = F_j(t) \quad \text{for} \quad t \leq T, \qquad (1)$$

$$F_j^P = F_j(t) \quad \text{for} \quad T < t \leq 2T. \qquad (2)$$

With the two focused signals separated, the nonlinear contribution F_j^{NL} can be found from the simple addition of these two signals.

$$F_j^{NL} = F_j^I + F_j^P. \qquad (3)$$

As shown by Sutin *et al.*,[10] the linear portions of the signals F_j^I and F_j^P are unaffected by the phase inversion process and thus sum to 0. As the nonlinear signals (actually only the second harmonics, the dominant signal remaining) are proportional to the square of the drive amplitude, i.e., $A_{2f} \propto A_f^2$,[6] this relationship dictates that the nonlinear response due to any signal will be identical to that produced by the phase inverted version of the same signal.[11] It follows that the resulting F_j^{NL} is the harmonic generated signal as a result of the large amplitude of the focused signals F_j^I and F_j^P.

To construct an image from the nonlinear response it is sufficient to simply take the maximum amplitude (A_{2f}) of the signals F_j^{NL} for all j and plot the values in a two-dimensional contour plot. This does provide an adequate image, but as the nonlinear response is dependent on the square of the linear signal amplitude (A_f^2), it is necessary to normalize each of the A_{2f} by the corresponding A_f^2. The images provided herein have been normalized in this fashion to produce the most accurate depiction of the localized nonlinear response.

Presented here in Fig. 2 are the results of performing both time reversed elastic nonlinearity diagnostic (TREND), as described above, and a standard linear ultrasound nondestructive evaluation method (C scan). It is readily apparent that there are large differences between the two images. It is our hypothesis that the differences between the two images result from the types of features to which each method is
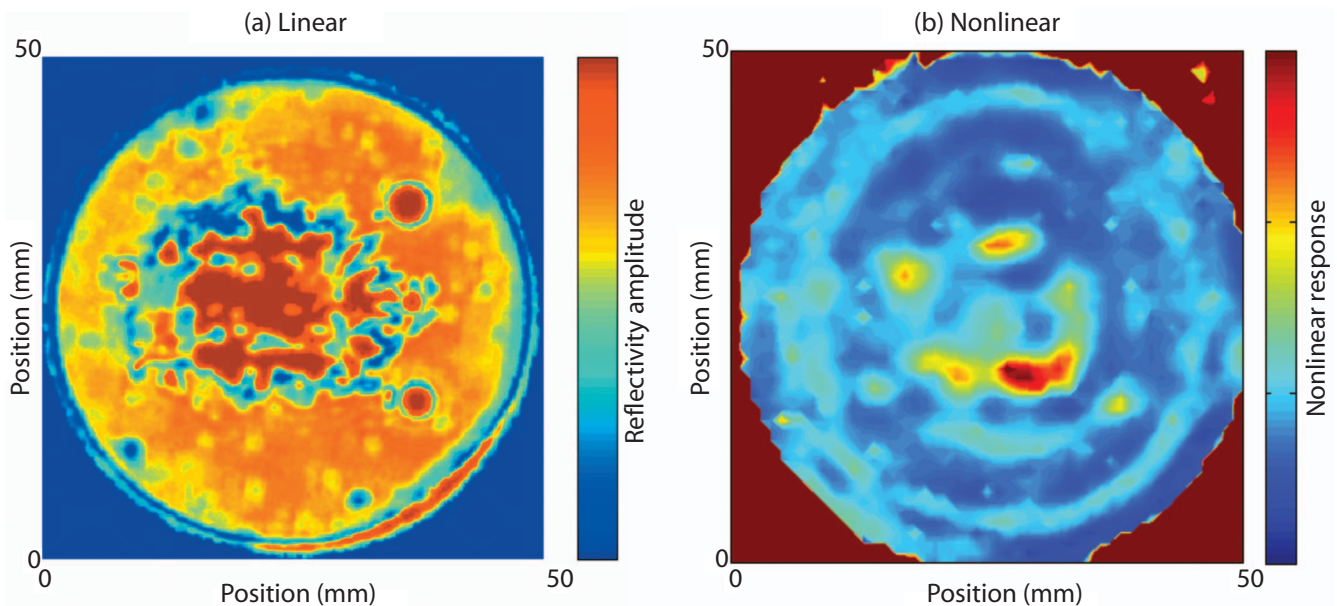

FIG. 2. (Color) Ultrasonic images, linear C scan (left) performed at 15 MHz, and nonlinear TREND scan (right) performed at 200 kHz. Dark red areas in the linear image indicate regions of acoustic impedance contrast (potential voids). Yellow to red regions in the TREND image indicate areas exhibiting a large nonlinear response (a suspected cracked or disbonded region).
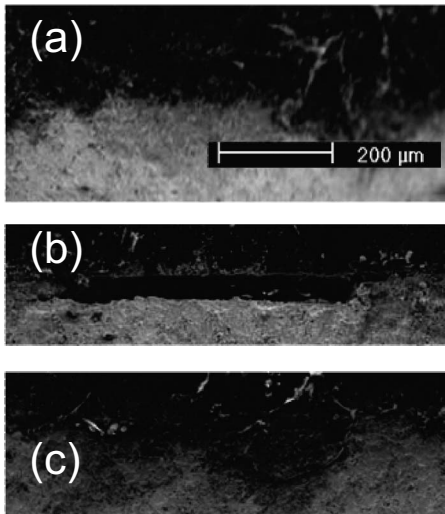
FIG. 3. SEM photographs taken of the bond at three locations: (a) good diffusion bond (no impedance contrast, no nonlinear response), (b) open void (large impedance contrast, no nonlinear response), and (c) interfacial disbonding (some impedance contrast, large nonlinear response).

sensitive, and therefore can "see." The linear method is known to measure impedance contrasts. Large impedance contrasts are found at open interfaces (e.g., voids and free surfaces). Small "tight" features (e.g., cracks and delaminations) may be missed by the linear methods, if too low frequency is used or appear as voids, when using high frequencies. The opposite is true for nonlinear techniques. One mechanism for the generation of a nonlinear response is the "clapping" of two surfaces in contact.[12–14] Separations that are larger than the imposed strains will not come into contact and thus will not produce a nonlinear response, though the acoustic impedance change may be high. Rather the nonlinear response will only be generated for interfaces in intimate contact. Also, nonlinear response can be generated where there are localized decreases in the elasticity of the material (i.e., weak portions of the material). In some cases the nonlinear method may be used to discriminate between different types of features and at other times may find features that the linear techniques fail to see at all.

TR was used to excite only the region of interest, thus not distorting the nonlinear image with nonlinear signals propagating from nearby locations. Constructing the signal for TR from impulse response functions taken from the samples response to a chirp provides an easy method for defining a frequency band of interest. Finally, applying the idea of phase inversion enhanced the ability to detect the nonlinear response (and remove some system nonlinearities). Combining these techniques result in a powerful tool for detecting near-surface mechanical damage, including disbonds.

From comparing the linear and nonlinear images (Fig. 2), we can see that the two techniques are "seeing" different features. Further investigation into the types of features [employing scanning electron microscopy (SEM), Fig. 3] reveals that, as conjectured, the linear method images large gaps, while the nonlinear technique sees the thin cracks. Further, the bond strength at the location of the voids can be assumed to be 0, while at the locations of the disbonding there may still be some strength. This was confirmed qualitatively and mechanical tests are currently underway to quantify the bond strengths at various points.

[1] M. Fink, Phys. Today **50**(3), 34 (1997).
[2] B. E. Anderson, C. Larmat, M. G. Griffa, T. J. Ulrich, and P. A. Johnson, Acoustics Today **4**, 5 (2008).
[3] A. M. Sutin, J. A. TenCate, and P. A. Johnson, J. Acoust. Soc. Am. **116**, 2779 (2004).
[4] C. Draeger, J.-C. Aime, and M. Fink, J. Acoust. Soc. Am. **105**, 618 (1999).
[5] P. A. Johnson, Mater. World **7**, 544 (1999).
[6] K. E.-A. Van Den Abeele, P. A. Johnson, and A. Sutin, Res. Nondestruct. Eval. **12**, 17 (2000).
[7] T. J. Ulrich, A. M. Sutin, and P. A. Johnson, J. Acoust. Soc. Am. **119**, 1514 (2006).
[8] T. J. Ulrich, A. M. Sutin, and P. A. Johnson, *Review of Quantitative Nondestructive Evaluation*, edited by D. O. Thompson and D. E. Chimenti (2006), Vol. 26.
[9] T. J. Ulrich, R. A. Guyer, and P. A. Johnson, Phys. Rev. Lett. **98**, 104301 (2007).
[10] A. Sutin, B. Libbey, V. Kurtenoks, D. Fenneman, and A. Sarvazyan, Proc. SPIE **6217**, 6217B-1 (2006).
[11] S. Krishnan and M. O'Donnell, Ultrason. Imaging **18**, 77 (1996).
[12] I. Solodov, N. Krohn, and G. Busse, Ultrasonics **40**, 621 (2002).
[13] I. Solodov, J. Wackerl, K. Pfleiderer, and G. Busse, Appl. Phys. Lett. **84**, 5386 (2004).
[14] O. Buck, W. Morris, and J. Richardson, Appl. Phys. Lett. **33**, 371 (1978).